# mTORC1 Promotes T-bet Phosphorylation To Regulate Th1 Differentiation

**Olesya Chornoguz,[*,†,‡,§] Robert S. Hagan,[*,†,‡,¶] Azeb Haile,[*,†,‡] Matthew L. Arwood,[*,†,‡] Christopher J. Gamper,[*,†,‡] Arnob Banerjee,[‖,#] and Jonathan D. Powell[*,†,‡]**

**CD4$^+$ T cells lacking the mTORC1 activator Rheb fail to secrete IFN-γ under Th1 polarizing conditions. We hypothesized that this phenotype is due to defects in regulation of the canonical Th1 transcription factor T-bet at the level of protein phosphorylation downstream of mTORC1. To test this hypothesis, we employed targeted mass-spectrometry proteomic analysis–multiple reaction monitoring mass spectrometry. We used this method to detect and quantify predicted phosphopeptides derived from T-bet. By analyzing activated murine wild-type and Rheb-deficient CD4$^+$ T cells, as well as murine CD4$^+$ T cells activated in the presence of rapamycin, a pharmacologic inhibitor of mTORC1, we were able to identify six T-bet phosphorylation sites. Five of these are novel, and four sites are consistently dephosphorylated in both Rheb-deficient CD4$^+$ T cells and T cells treated with rapamycin, suggesting mTORC1 signaling controls their phosphorylation. Alanine mutagenesis of each of the six phosphorylation sites was tested for the ability to impair IFN-γ expression. Single phosphorylation site mutants still support induction of IFN-γ expression; however, simultaneous mutation of three of the mTORC1-dependent sites results in significantly reduced IFN-γ expression. The reduced activity of the triple mutant T-bet is associated with its failure to recruit chromatin remodeling complexes to the *Ifng* gene promoter. These results establish a novel mechanism by which mTORC1 regulates Th1 differentiation, through control of T-bet phosphorylation.** ***The Journal of Immunology*****, 2017, 198: 3939–3948.**

The CD4$^+$ T helper lymphocytes modulate immune response to intracellular and extracellular pathogens, provide help to B cells, and play an important role in immune response to tumors. Upon activation, CD4$^+$ T helper lymphocytes differentiate into effector T cells (Th1, Th2, Th17, T follicular helper, and T regulatory cells) with restricted patterns of cytokine expression and functional specificity (1). These subsets have unique roles during specific classes of adaptive immune responses and each is characterized by expression of critical lineage-determining transcription factors such as T-bet, GATA3, RORγT, Foxp3, and Bcl-6 for Th1, Th2, Th17, T regulatory, and T follicular helper cells, respectively. Among important signals directing Th cell differentiation are the cytokines present in the milieu during Th cell activation. Many cytokines direct CD4$^+$ T cell differentiation by binding to their cognate receptors and activating STAT family transcription factors (2). When a naive CD4$^+$ T cell is activated in the presence of IL-12 and IFN-γ and in the absence of IL-4, it becomes a Th1 cell. During the initial phase of differentiation, TCR and IFN-γ–induced STAT1-signaling pathways synergize to induce T-bet expression, a T-box family transcription factor that is critical for Th1 differentiation (3). In the later stages of differentiation, IL-12–induced STAT4 signaling sustains T-bet expression in the absence of TCR stimulation (4). Although molecular mediators necessary for Th cell differentiation are well studied, the mechanisms of how these molecular mediators are regulated remains incompletely understood.

Recent studies demonstrated that the kinase mTOR (known as mammalian target of rapamycin) integrates environmental cues provided by nutrients, cytokines, and costimulatory signals present in the immune microenvironment and helps to promote Th cell differentiation (5–7). mTOR is a highly conserved serine/threonine kinase of the PI3K family that exists as a part of two complexes, mTORC1 and mTORC2. The mTORC1 complex is characterized by the scaffold protein Raptor and is activated by the small GTPase Rheb (8). Rapamycin, a macrolide antibiotic and immunosuppressive agent, inhibits mTORC1. We, and others (6, 9, 10), have recently shown that mTORC1 and mTORC2 have differential contributions to T helper differentiation. For example, in the absence of Rheb and hence low mTORC1 activity, CD4$^+$ T cells fail to differentiate into Th1 and Th17 subsets; however, they are capable of differentiating into Th2 cells. Furthermore, inhibiting mTORC1 with rapamycin also causes a defect in Th1 differentiation.

The transcription factor T-bet plays a critical role in Th1 differentiation (3). One mechanism by which T-bet controls the ex-

*Department of Oncology, Johns Hopkins University School of Medicine, Baltimore, MD 21287; †Bloomberg-Kimmel Institute for Cancer Immunotherapy, Johns Hopkins University School of Medicine, Baltimore, MD 21287; ‡Sidney Kimmel Comprehensive Cancer Center, Johns Hopkins School of Medicine, MD 21287; §Janssen Research and Development, Department of Biologics Research, Spring House, PA 19477; ¶Division of Pulmonary Diseases and Critical Care Medicine, Department of Medicine, University of North Carolina, Chapel Hill, NC 27599; ‖Program in Oncology, University of Maryland Marlene and Stewart Greenebaum Comprehensive Cancer Center, Baltimore, MD 21201; and #Department of Medicine, University of Maryland School of Medicine, Baltimore, MD 21201

ORCIDs: 0000-0002-1504-0086 (R.S.H.); 0000-0003-0253-2177 (C.J.G.).

Received for publication June 21, 2016. Accepted for publication March 21, 2017.

This work was supported by National Institutes of Health Grants R01 AI077610-07 (to J.D.P.) and KO8HL093027 (to A.B.).

Address correspondence and reprint requests to Dr. Jonathan D. Powell, Johns Hopkins University School of Medicine, 1650 Orleans Street, Bunting-Blaustein Cancer Research Building Room 443, Baltimore, MD 21287. E-mail address: poweljo@jhmi.edu

The online version of this article contains supplemental material.

Abbreviations used in this article: ChIP, chromatin immunoprecipitation; EV, empty vector; ICS, intracellular cytokine staining; KO, knockout; LC-MRM-MS, liquid chromatography multiple reaction monitoring mass spectrometry; MRM, multiple reaction monitoring; MRM-MS, multiple reaction monitoring mass spectrometry; WT, wild-type.

pression of its target genes is by recruiting cellular machinery that conveys permissive and removes prohibitive epigenetic modifications, leading to gene transcription (11). Specifically, T-bet interacts with a histone demethylase complex Jmjd3 that removes repressive methylation H3K27 and histone methyltransferase complex Set7/9 that adds permissive H3K4Me2 methylation. T-bet promotes transcription of the essential Th1 genes such as IFN-γ, TNF-α, and CXCR3 and represses transcription of the Th2 and Th17 lineage-determining transcription factors GATA3 and RORγt (4, 12). Although our laboratory has previously demonstrated that mTORC1 is pivotal for Th1 differentiation (6), a link between mTORC1 signaling and T-bet activity has yet to be defined.

T-bet has been shown to undergo several types of posttranslational modifications including phosphorylation and ubiquitination (13, 14). T-bet phosphorylations at residues T302 and S508 are involved in suppression of IL-2 production (14, 15); Y219/Y265/Y304 triple phosphorylation by c-Abl tyrosine kinase regulates T-bet's ability to bind to DNA of its target genes and promotes gene expression (16). Y304 is crucial for T-bet's interaction with RUNX1 transcription factor and inhibition of Th17 differentiation (17). In light of the importance of these phosphorylation events on the regulation of T-bet function (13–17), we hypothesized that mTORC1 may also control T-bet's activity via regulation of T-bet phosphorylation.

To test this hypothesis, we developed a targeted mass spectrometry method that allows fast, reliable, and accurate phosphorylated peptide detection and quantitation. Most current proteomic methods for discovery of novel phosphorylations include an enrichment step for phosphorylated peptides and subsequent global proteomic analysis (18). Liquid chromatography multiple reaction monitoring mass spectrometry (LC-MRM-MS) can reproducibly detect low quantities of phosphorylated peptides from complex biological samples without additional enrichment due to the capability of specifically selecting only the peptide of interest among a complex matrix (19, 20). We developed an LC-MRM-MS workflow to investigate whether mTORC1 controls T-bet through phosphorylation. We discovered five novel T-bet phosphorylations and established that four of these novel phosphorylations are mTORC1 dependent. Three of the mTORC1-dependent phosphorylations influence T-bet's

A

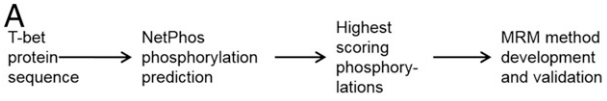


B

| Phoshorylation sites | Peptide Sequence | NetPhos score | Detected in initial MRM screen | Previously published |
|---|---|---|---|---|
| S52 | AGS**S**LGTPYSGGALVPAAPGR [48, 68] | 0.985 | Yes | No |
| T55 | AGSSLG**T**PYSGGALVPAAPGR [48, 68] | 0.677 | No | No |
| S52, T55 | AGS**S**LG**T**PYSGGALVPAAPGR [48, 68] | N/A | Yes | No |
| Y76 | FLGSFA**Y**PPR [69, 78] | 0.034 | Yes | No |
| Y117 | AGL**Y**PGPR[113, 120] | 0.109 | Yes | No |
| S224 | LYVHPD**S**PNTGAHWMR [217, 232] | 0.885 | Yes | No |
| S508 | ISPYPSSGDSS**S**PAGAPSPFDK [496, 517] | 0.818 | Yes | Yes |
| S508, S523 | ISPYPSSGDSS**S**PAGAP**S**PFDK [496, 517] | N/A | No | No |

**FIGURE 1.** Proteomic workflow for discovery and validation of novel T-bet phosphorylation sites. (**A**), Mouse T-bet protein sequence was used as an input for phosphorylation site prediction analysis using NetPhos program. T-bet phosphorylations with the highest predicted scores were chosen for LC-MRM-MS method development. (**B**) Phosphorylation sites and their NetPhos scores that were chosen for preliminary MRM method development.

A


B

| # | Site | Peptide sequence |
|---|---|---|
| 1 | S52 | AGS**S**LGTPYSGGALVPAAPGR [48, 68] |
| 2 | T55 | AGSSLG**T**PYSGGALVPAAPGR [48, 68] |
| 3 | Y76 | FLGSFA**Y**PPR [69, 78] |
| 4 | Y117 | AGL**Y**PGPR [113, 120] |
| 5 | S224 | LYVHPD**S**PNTGAHWMR [217, 232] |
| 6 | S508 | ISPYPSSGDSS**S**PAGAPSPFDK [496, 517] (Hwang et al, J. Exp. Med, 2005) |

**FIGURE 2.** Six phosphorylation sites were detected and validated using MRM-MS. (**A**) Schematic of T-bet protein with T-box DNA-binding domain shown as a gray rectangle in the middle. The numbers in gray circles show the location of the six different phosphorylations on the T-bet sequence. (**B**) List of the six phosphorylations detected using MRM-MS and their corresponding tryptic peptides. Five of these phosphorylations are novel and one has been previously published (15).

ability to induce IFN-γ production in EL4 and T-bet knockout (KO) $CD4^+$ T cells. Furthermore, simultaneous mutation of three mTORC1-dependent phosphorylation sites impaired T-bet's ability to recruit chromatin-remodeling complexes to *Ifng* promoter, as shown by a reduction in the permissive H3K4Me2 epigenetic mark at the promoter following mutant T-bet overexpression.

## Materials and Methods

### *Chemicals and Abs*

All reagents and chemicals were purchased from Sigma Aldrich unless noted otherwise. Rapigest detergent was purchased from Waters. Anti-GFP Alexa 488 Ab was purchased from Santa Cruz and mouse anti–IFN-γ APC Ab was purchased from eBioscience. IFN-γ ELISA kit was purchased from R&D Systems.

### *Mice*

$Rheb^{fl/fl}$ mice were obtained from Dr. P. Worley (The Johns Hopkins University, Baltimore) and were crossed with $CD4^{Cre}$ mice obtained from the Jackson Laboratory to obtain $Rheb^{fl/fl}$ $CD4^{Cre}$ mice with T cell–specific deletion of Rheb (21). Wild-type (WT) C57/BL6 mice were obtained from the Jackson Laboratory and were bred and maintained at Johns Hopkins University animal facility. All animal protocols were approved by the Johns Hopkins Institutional Animal Care and Use Committee.

### *T cell activation and in vitro Th1 differentiation*

$CD4^+$ T cells were purified from spleens and lymph nodes of WT C57/BL6 and $CD4^{Cre}$ $Rheb^{fl/fl}$ mice using Miltenyi $CD4^+$ T cell negative selection purification kit. Purified $CD4^+$ T cells (87–95% purity) were plated into six-well plates coated with 3 μg/ml of anti-CD3 Ab at 2–5 × $10^6$ cells per well. T cell cultures were supplemented with 2 μg/ml soluble anti-CD28, 50 ng/ml IFN-γ, 10 ng/ml IL-12, and 1 μg/ml anti–IL-4 Ab. Some of the WT T cell cultures were supplemented with 500 nM rapamycin. These T cells were then cultured either 24 or 48 h in the 6% $CO_2$, 37°C tissue culture incubator. $CD4^+$ T cells were harvested and the cell pellets were snap frozen in liquid nitrogen and stored at −80°C until LC-MRM-MS analysis.

### *Sample preparation for mass spectrometry analysis*

T cell samples were prepared using a previously described Rapigest mass spectrometry protocol (22) with several modifications. Frozen pellets were thawed on ice and lysed with 0.15% Rapigest (Waters) in 100 mM $NH_4HCO_3$ (pH 8.4) supplemented with phosphatase inhibitors 10 mM $Na_4O_7P_2$, 50 mM NaF, and 1 mM $Na_3VO_4$. Protein

concentration of resulting lysates was measured by Bradford assay and proteins were digested overnight with sequencing grade modified trypsin (Promega) at 1:50 trypsin:protein ratio. Digested samples were acidified to pH 2.5–3 by 10% trifluoroacetic acid then incubated at 37°C for 1 h. Next the samples were snap frozen in liquid nitrogen and allowed to thaw at room temperature to promote Rapigest precipitation. Then samples were microcentrifuged at 15,000 rpm for 10 min to pellet precipitated Rapigest. Supernatants containing tryptic peptides were removed and their pH was brought to 7.5–8 using 10% ammonium hydroxide. Peptide concentration was measured using OD280 on a Nanodrop spectrophotometer. Then peptides were desalted using Pierce C18 spin columns (Thermo Fisher Scientific) according to the manufacturer's protocol. Desalted peptides were lyophilized and stored at −20°C until LC-MRM-MS analysis.

### *LC-MRM-MS*

A list of predicted tryptic peptides containing phosphorylation sites of interest was generated using open source Skyline (23) software (McCoss Laboratory, University of Washington). Peptides and their transitions were imported into AB Sciex Analyst software to generate methods for AB Sciex 5500 triple quadrupole mass spectrometer. For every peptide, 4–5 transitions (fragments) of the highest signal-to-noise ratio were chosen for quantitation study.

Ninety micrograms of peptides were loaded on to the column and analyzed on AB Sciex 5500 triple quadrupole mass spectrometer interfaced with Shimadzu UFLC (an ultra flow liquid chromatographer). Peptides were separated on a Waters C18 Acquity BEH 1.7 μm, 1.0 × 50 $mm^2$ column using the following 30 min gradient (24) of mobile phases A and B: 5% mobile phase B for 2 min, then mobile phase B was increased to 60% from minute 2 to 26, followed by an increase to 98% B from minute 26 to 27, then maintained at 5% B from minute 27 to 30. Mobile phase A was 0.1% formic acid in LC-MS grade $H_2O$. Mobile phase B was 0.1% formic acid in 90% acetonitrile. Column compartment was heated to 40°C.

### *Site-directed mutagenesis of T-bet*

Mouse WT T-bet in the MigR1 retroviral vector has been previously described (25, 26). All of the mutants (shown in Fig. 5A) were made using the QuikChange Lightning site-directed mutagenesis kit (Stratagene) according to the manufacturer's protocol. Mutagenesis was verified by sequencing. Triple mutant creation and sequencing verification was conducted by GenScript.

### *EL4 transfection*

EL4 cells were maintained in RPMI with 10% FBS and antibiotics, subsequently noted as EL4 media. EL4 transfections were performed by electroporating 5 × $10^6$ cells with 15 μg of mutant or WT T-bet containing MigR1 vector. Transfection efficiency was monitored by percentage GFP expression using flow cytometry. For IFN-γ production measurements percentage of $GFP^+$ EL4 cells was measured by flow cytometry and 0.8–1 × $10^5$ $GFP^+$ cells were plated per well of a 24-well plate in 800 μL of EL4 media. Cells were activated with PMA/ionomycin, and 24 h later supernatants were collected and IFN-γ amount was measured by ELISA. For intracellular cytokine staining (ICS) transfected EL4 cells were plated in round-bottom 96-well plates and stimulated with PMA/ionomycin in the presence of GolgiPlug (BD Biosciences) overnight. Stimulated cells were harvested and fixed using BD Fix/Perm reagent and later stained for IFN-γ in BD Perm/Wash solution.

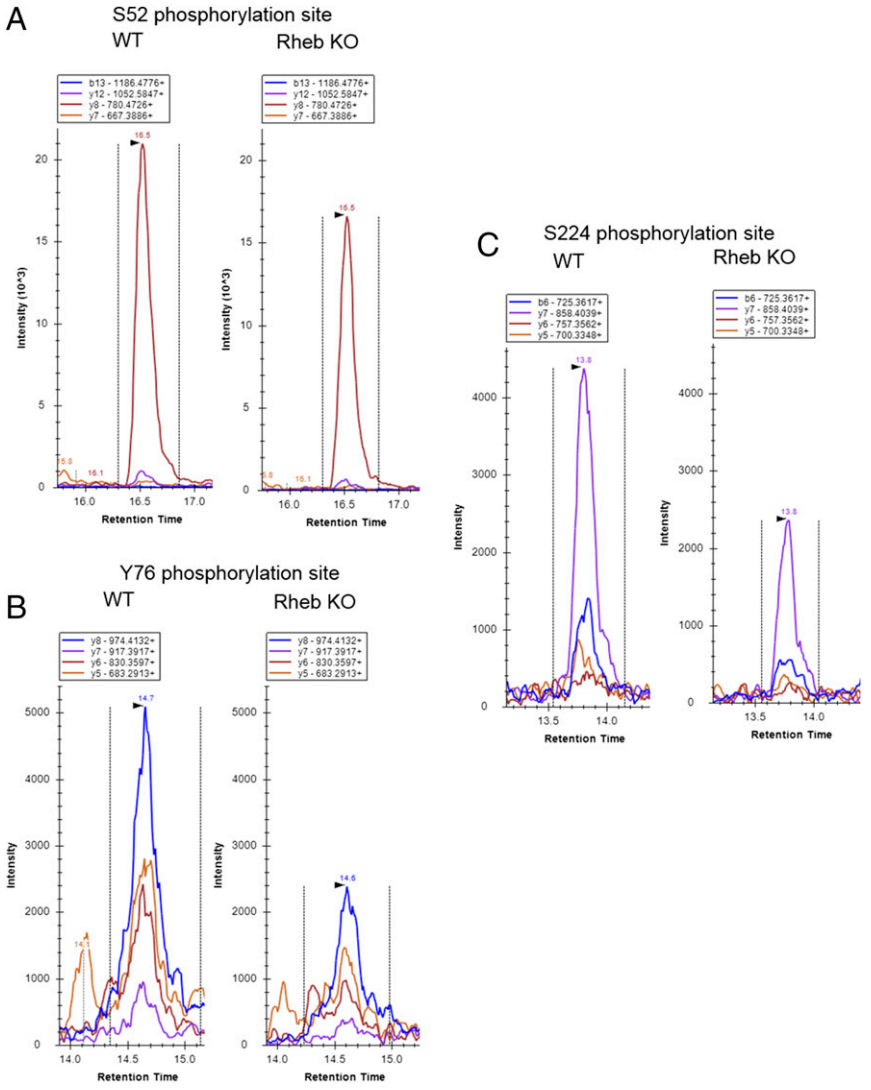


**FIGURE 3.** LC-MRM-MS traces of T-bet peptides that contain phosphorylations regulated by mTORC1. Different color traces represent different fragments of the same peptide. The fragments are denoted at the top of each LC-MRM-MS trace. (**A**) S52 phosphorylation site, peptide AGS**S**LGTPYSGGALVPAAPGR, (**B**) Y76 phosphorylation site, peptide FLGSFA**Y**PPR, (**C**) S224 phosphorylation site, peptide LYVHPD**S**PNTGAHWMR. Data are representative of five individual experiments.

*Retroviral transduction of CD4$^+$ T cells*

MigR1 plasmids encoding an empty vector (EV), WT T-bet, or T-bet mutants were transiently transfected into the 293 Phoenix Eco (27) packaging cell line (obtained from American Type Culture Collection) using Lipofectamine 2000. Supernatants were collected at 48 and 72 h, pooled, and stored at 4˚C until use. CD4$^+$ T cells were isolated from spleens and lymph nodes of T-bet KO mice (28). T cells were activated with 3 μg/ml plate-bound anti-CD3, 2 μg/ml soluble anti-CD28 Ab, and 1 ng/ml IL-2 for 48 h. Then activated T cells were harvested, resuspended in fresh T cell media, retrovirus-containing supernatant, and transferred into retronectin-coated 24-well plates. CD4$^+$ T cells were spinfected in 24-well plates for 2 h at 2500 rpm then resuspended in fresh T cell media with IL-2 (1 ng/ml), IL-12 (10 ng/ml), and anti–IL-4 Ab (1 μg/ml). Transduced T cells were harvested after 48 h and assayed for IFN-γ production by ELISA and T-bet expression by flow cytometry.

*Chromatin immunoprecipitation*

A total of $3.5 \times 10^6$ cells expressing vectors containing WT, EV, and triple mutant T-bet were resuspended in media at $10^7$/ml, crosslinked with formaldehyde (1% final concentration), washed, and lysed using the Magna ChIP A/G Chromatin Immunoprecipitation Kit (EMD Millipore, Billerica, MA) according to the manufacturer's instructions. Nuclei were pelleted and subjected to sonication. The optimized condition to shear the chromatin was two cycles (5 min each) of 30 s sonication followed by 30 s of rest for a total of 10 min using Bioruptor 300 (Diagenode, Denville, NJ). For chromatin immunoprecipitation (ChIP), 50 μl chromatin aliquot was incubated either with 10 μg of rabbit anti-dimethyl-histone H3K4Me2 (EMD Millipore) or 2 μg of normal rabbit IgG Ab (Santa Cruz Biotechnology, Santa Cruz). ChIP-grade protein A/G magnetic beads (20 μl) were added to each and were incubated on a rotator overnight at 4˚C. ChIP samples were washed following the Magna ChIP protocol. Protein/DNA complexes were eluted, crosslinks reversed, and DNA was purified by phenol/chloroform extraction and precipitation. Quantitative PCR was performed using SYBR Green Master Mix (Applied Biosystems, Warrington, U.K.). For DNA quantification, a standard curve was generated by serial dilution of purified mouse genomic DNA (Promega, Madison, WI). All ChIP samples were normalized to 2% input.

*Luciferase assay*

Plasmids including a pGL3 luciferase reporter controlled by the SOCS3 promoter and an expression vector encoding murine Bcl-6 were generously provided by Amy Weinmann (University of Alabama at Birmingham) (29). EL4 cells were transfected by electroporation as noted above using 10 μg of MIGR1 T-bet expression vector with or without 10 μg of Bcl-6 expression vector and 3 μg of pGL3 SOCS3 reporter, 3 μg of pRLtk vector encoding Renilla luciferase (Promega), and 1 μg of pMAX GFP (Lonza, Basel, Switzerland). Total plasmid DNA per transfection was normalized by MIGR1 plasmid without an expression insert. Cells were harvested 18–24 h posttransfection and cultured with PMA and ionomycin for 6 h before measuring firefly and Renilla luciferase activities using the Dual Glo Luciferase kit (Promega). Firefly luciferase activity was normalized to Renilla luciferase activity and is presented as fold induction compared with EV control.

## Results

*Development of a workflow for novel phosphorylation site discovery*

To discover novel T-bet phosphorylations and test our hypothesis that mTORC1 controls T-bet function through phosphorylation, we developed a hypothesis-driven targeted mass spectrometry work-

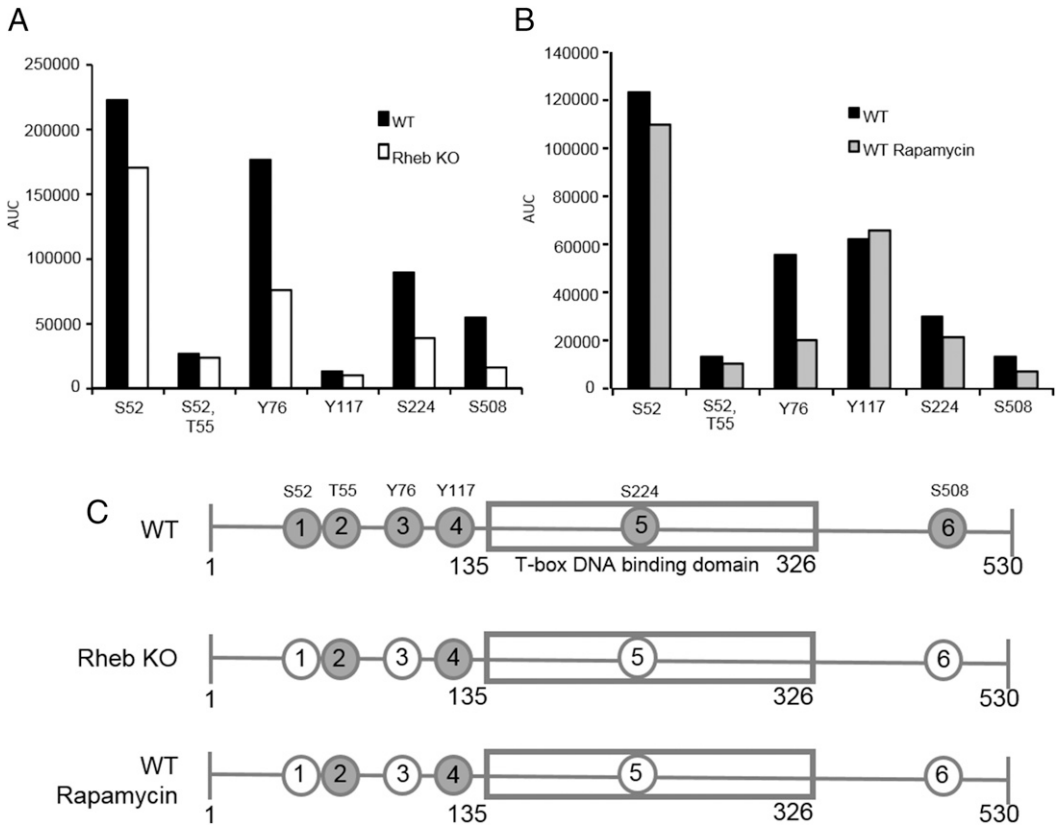


**FIGURE 4.** Three of the novel T-bet phosphorylations are mTORC1 dependent. (**A**) WT C57/BL6 (WT) or Rheb$^{fl/fl}$ CD4$^{Cre}$ (Rheb KO) CD4$^+$ T cells were purified from spleens and lymph nodes of 6–12-wk-old mice and activated with plate-bound anti-CD3 and soluble anti-CD28 for 24 h in Th1 polarizing culture conditions. Activated T cells were harvested, lysed with Rapigest, trypsin digested, and analyzed by LC-MRM-MS. Area under the curve (AUC) on the *y*-axis is the measure of phosphorylated peptide abundance. Data are from one of two experiments with T cells from individual mice. (**B**) CD4$^+$ T cells were purified from spleens and lymph nodes of WT mice and activated for 48 h as in (A) in the presence or absence of 500 nM rapamycin (WT or WT rapamycin), prepared and analyzed as in (A). Data are from one of three experiments with T cells from individual mice. (**C**) Schematic of T-bet with phosphorylations shown as circles with numbers. Gray circles are the phosphorylation sites. White circles show phosphorylations that are mTORC1 dependent. Data are from one of five experiments with T cells from individual mice.

flow (Fig. 1A). Because MRM requires a priori knowledge of peptides and phosphorylation sites within the protein of interest, we used the NetPhos phosphorylation prediction algorithm (30) to identify target peptides with predicted phosphorylation sites. We selected eight peptides containing a total of 10 potential phosphorylation sites for a preliminary MRM screen (Fig. 1B). Because NetPhos cannot always accurately predict true phosphorylation sites a few phosphorylation sites with low NetPhos prediction scores were included in the preliminary screen. One of these phosphorylation sites (S508) was previously published (15) and was included to validate method development. To validate T-bet peptide identifications all six of the phosphorylated peptides and two of their unphosphorylated counterparts detected by MRM were validated by comparing the elution time and fragmentation pattern of peptides detected in T cell samples to elution time and fragmentation pattern of corresponding synthetic phosphorylated and unphosphorylated peptides (data not shown).

*Identification of five novel T-bet phosphorylation sites*

Using the workflow that combined NetPhos phosphorylation prediction together with LC-MRM-MS we were able to detect 6 out of the 10 phosphorylation sites examined. These six phosphorylation sites, including S508, were consistently detected by MRM in T cells from WT C57/BL6 cultured in Th1 conditions and peptides containing these phosphorylations were chosen for further studies (Fig. 2). Most of these sites (S52, T55, Y76, and Y117) are located in the N terminus of T-bet (Fig. 2A). Interestingly, Y76 phosphorylation has been computationally predicted as a possible site of c-Abl phosphorylation, but was not confirmed experimentally (31). We were able to confirm that Y76 phosphorylation takes place using MRM-MS. One of the phosphorylation sites, S224, is located within the T-box DNA-binding domain and S508 is located in the C-terminal region of T-bet. Two additional phosphorylation sites, Y76 and Y117, are located in the domain of T-bet that is responsible for T-bet's interaction, with histone demethylase complex Jmjd3 that removes repressive methylation H3K27 and histone methyltransferase complex Set7/9 that adds permissive H3K4Me2 methylation (32–34). Therefore, by combining the phosphorylation prediction tool and targeted mass spectrometry workflow, we were able to discover novel T-bet phosphorylation sites.

*Four out of five of the novel phosphorylations are reduced in the absence of mTORC1 activity*

We hypothesized that mTORC1 signaling might control Th1 differentiation in part by regulating T-bet function through phosphorylation. To test this hypothesis, we conducted LC-MRM-MS analysis on Rheb-deficient $CD4^+$ T cells, as well as WT $CD4^+$

A

| # | Site | Mutation |
|---|---|---|
| 1 | S52 | S52A |
| 2 | T55 | T55A |
| 3 | Y76 | Y76A |
| 4 | Y117 | Y117A |
| 5 | S224 | S224A |
| 6 | S508 | S508A |

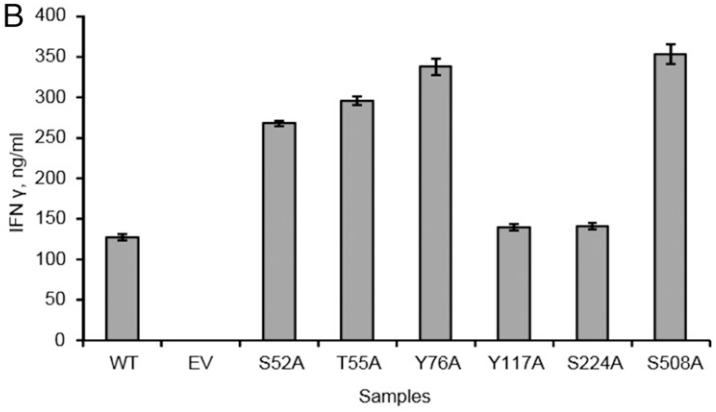


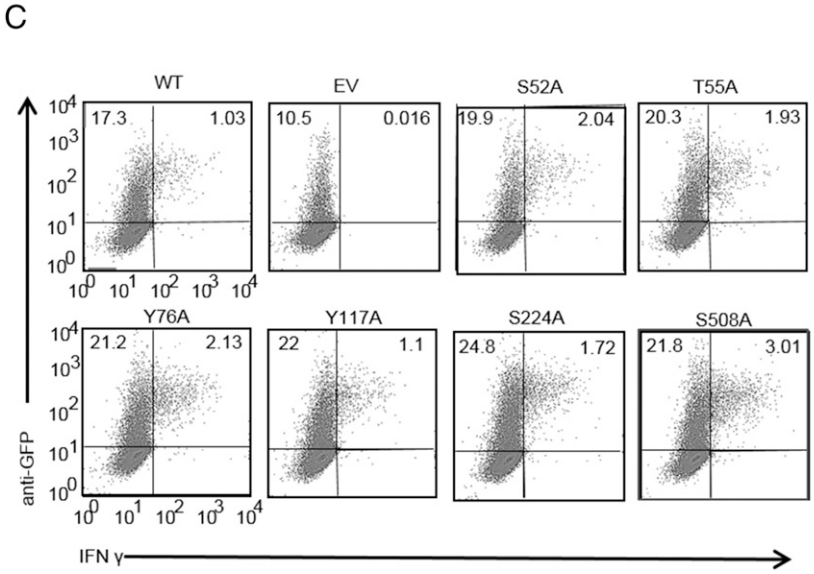


**FIGURE 5.** Single phosphorylation site T-bet mutants are not deficient in their ability to induce IFN-γ. (**A**) Six single phosphorylation site mutants. All of the phosphorylation sites were mutated to alanines. (**B**) EL4 cells were transfected with WT, EV, or different mutants. At 24 h posttransfection equal numbers of $GFP^+$ cells were plated and activated with PMA/ionomycin overnight. Supernatants were analyzed for IFN-γ by ELISA. Error bars are SEM. (**C**) EL4 cells transfected as in (B) and stimulated with PMA/ionomycin overnight in the presence of GolgiPlug protein transport inhibitor. Data are from one of three experiments.

T cells treated with rapamycin. MRM-MS analysis revealed that S52, Y76, S224, and S508 (Fig. 3) phosphorylations are consistently reduced when mTORC1 activity is abrogated (Figs. 3, 4). Fig. 3 shows LC-MRM-MS traces for peptides containing S52, Y76, and S224 phosphorylations. The abundance of these phosphorylations, as measured by the area under the curve for all fragments of a particular peptide, was consistently decreased (Fig. 4A, 4B). The abundance of the corresponding unphosphorylated peptides was similar for WT, Rheb KO, and WT treated with rapamycin samples (data not shown).

*Mutating single phosphorylation sites does not affect T-bet's ability to induce IFN-γ expression*

Published data (13, 14, 16) suggested that within T-bet, S52, Y76, and S224 phosphorylation sites could be important for T-bet's ability to induce IFN-γ expression by influencing its ability to bind DNA and/or interact with chromatin remodeling complexes. A distinct phosphorylation site, S508, has been previously demonstrated to be important for suppression of IL-2 production by T-bet (15).

To test the function of the six phosphorylation sites detected by MRM-MS, we created alanine substitution mutants for each individually (Fig. 5A). The best characterized function of T-bet is induction of IFN-γ expression. This can be modeled by transient overexpression of T-bet in the EL4 lymphoma cell line, which does not express T-bet or IFN-γ (3). T-bet expression in EL4 cells is both necessary and sufficient to induce IFN-γ, and such functional analyses in EL4 cells have correlated strongly with T-bet function in primary $CD4^+$ T cells (29, 33–35). We transfected EL4 cells with either WT T-bet or T-bet mutants and measured IFN-γ production by ICS and ELISA. All of the T-bet single site mutants were able to induce IFN-γ expression (Fig. 5B, 5C) as shown by ELISA and ICS. The level of IFN-γ induced by mutants was either similar or higher in magnitude as compared with the level of IFN-γ induced by WT T-bet. Therefore, mutating individual phosphorylation sites is not sufficient to reduce T-bet's ability to induce IFN-γ expression.

*Mutating three of the mTORC1-dependent phosphorylations reduces T-bet's ability to induce IFN-γ expression in EL4 and T-bet KO $CD4^+$ T cells*

Because S52, Y76, and S224 phosphorylations are mTORC1 dependent and are in the domains of T-bet that are important for T-bet's ability to induce its target gene expression (32–34), we hypothesized that mutating all three of these phosphorylations could impact T-bet's ability to promote IFN-γ expression. Therefore, we created a triple mutant T-bet in which each of the S52, Y76, and S224 phosphorylations were all simultaneously

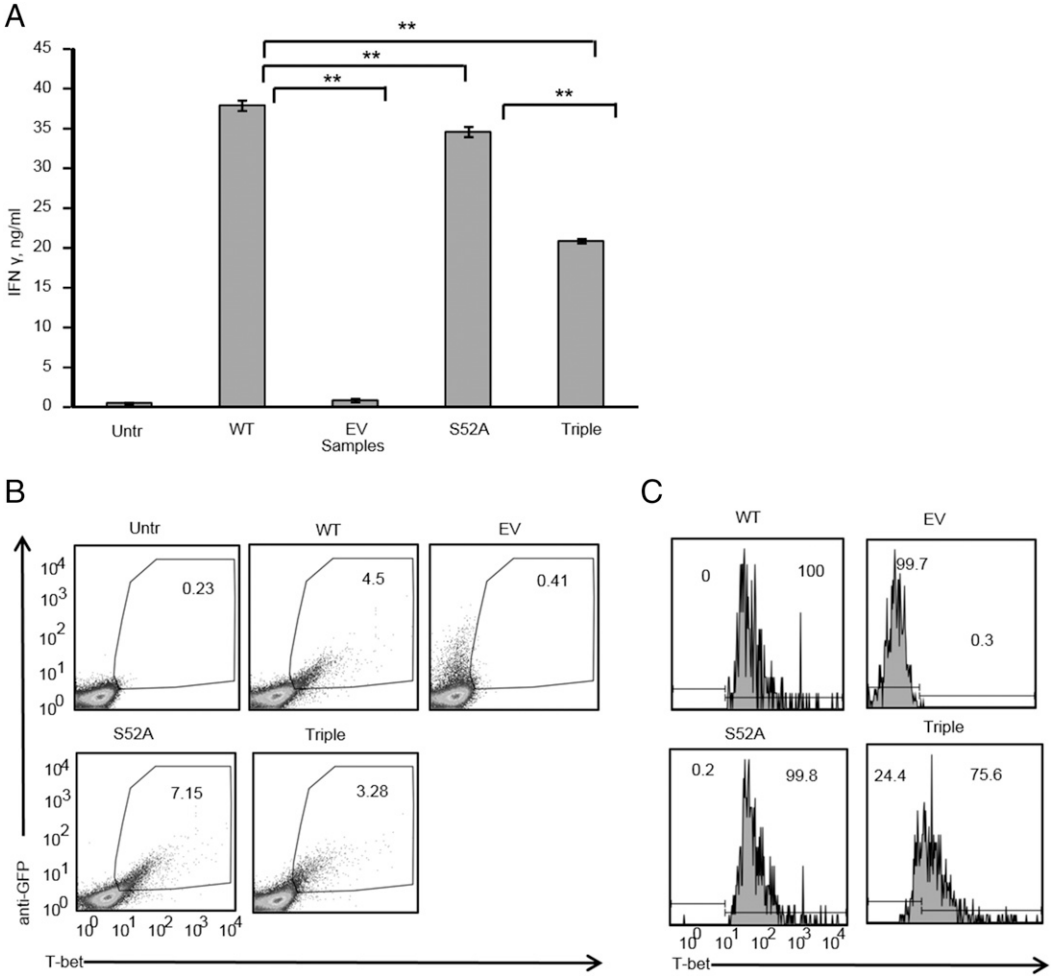


**FIGURE 6.** Triple phosphorylation site T-bet mutant has a significantly reduced ability to induce IFN-γ in EL4. (**A**) EL4 cells were transfected with WT, EV, S52A single phosphorylation site mutant, or triple phosphorylation site mutant. At 24 h posttransfection equal numbers of $GFP^+$ cells were plated and activated with PMA/ionomycin overnight. Supernatants were analyzed for IFN-γ by ELISA. Error bars are SEM, $^{**}p < 0.05$ by one-way ANOVA with Bonferroni multiple comparison test. (**B**) EL4 transfected as in (A) were fixed, permeabilized, and stained with anti-GFP and anti–T-bet Abs. (**C**) Samples from (B) gated on $GFP^+$ cells and T-bet levels are shown as histograms. Data are representative of four experiments.

mutated to alanine. The resulting triple mutant was transfected into EL4 cells and its ability to induce IFN-γ was compared with WT T-bet. Triple mutant T-bet has a significantly reduced ability to induce IFN-γ expression as compared with WT T-bet, as shown by either transient transfection via electroporation (Fig. 6A) or stable retroviral transduction (Supplemental Fig. 1A) of WT or triple mutant T-bet in EL4 cells. It should be noted that transfection efficiency and T-bet protein levels by Western blot and ICS were similar for WT and triple mutant T-bet over the course of multiple experiments (Fig. 6B, 6C, Supplemental Fig. 1). This is readily seen in the EL4 cells stably transfected with T-bet or the T-bet mutants (Supplemental Fig. 1). Having employed the EL4 cell line to identify the functional importance of the mTORC1-dependent phosphorylation sites, we next wanted to test the mutant T-bet constructs in primary $CD4^+$ T cells. To study the ability of the triple mutant to induce IFN-γ production in primary T cells we used $CD4^+$ T cells from T-bet KO mice. Of note, T-bet KO $CD4^+$ T cells have similar levels of Rheb protein and mTORC1 activity when compared with WT $CD4^+$ T cells (Supplemental Fig. 2). Furthermore, T-bet KO $CD4^+$ T cells are not globally deficient in their ability to secrete cytokines, because even though they do not secrete IFN-γ they secrete TNF-α at levels that are similar to WT $CD4^+$ T cells (Supplemental Fig. 3). T-bet KO $CD4^+$ T cells were transduced with retroviruses containing WT, triple mutant, EV, and S224A single phosphorylation site mutant constructs (Fig. 7). Similar to the EL4 experiments, we observed that the triple mutant has a significantly reduced ability to induce IFN-γ expression in T-bet KO $CD4^+$ T cells as compared with WT T-bet (Fig. 7A).

### *Triple mutant T-bet has an impaired ability to promote chromatin remodeling*

To understand why the triple mutant T-bet has a diminished ability to promote IFN-γ expression we investigated the triple mutant's ability to promote addition of the permissive chromatin mark H3K4Me2. The presence of this chromatin mark at *Ifng* promoter has been demonstrated to be exquisitely T-bet dependent in EL4 and primary T cells (32). Furthermore, EL4 cells have been successfully used to study chromatin remodeling induced by T-bet and these findings directly translated into chromatin remodeling

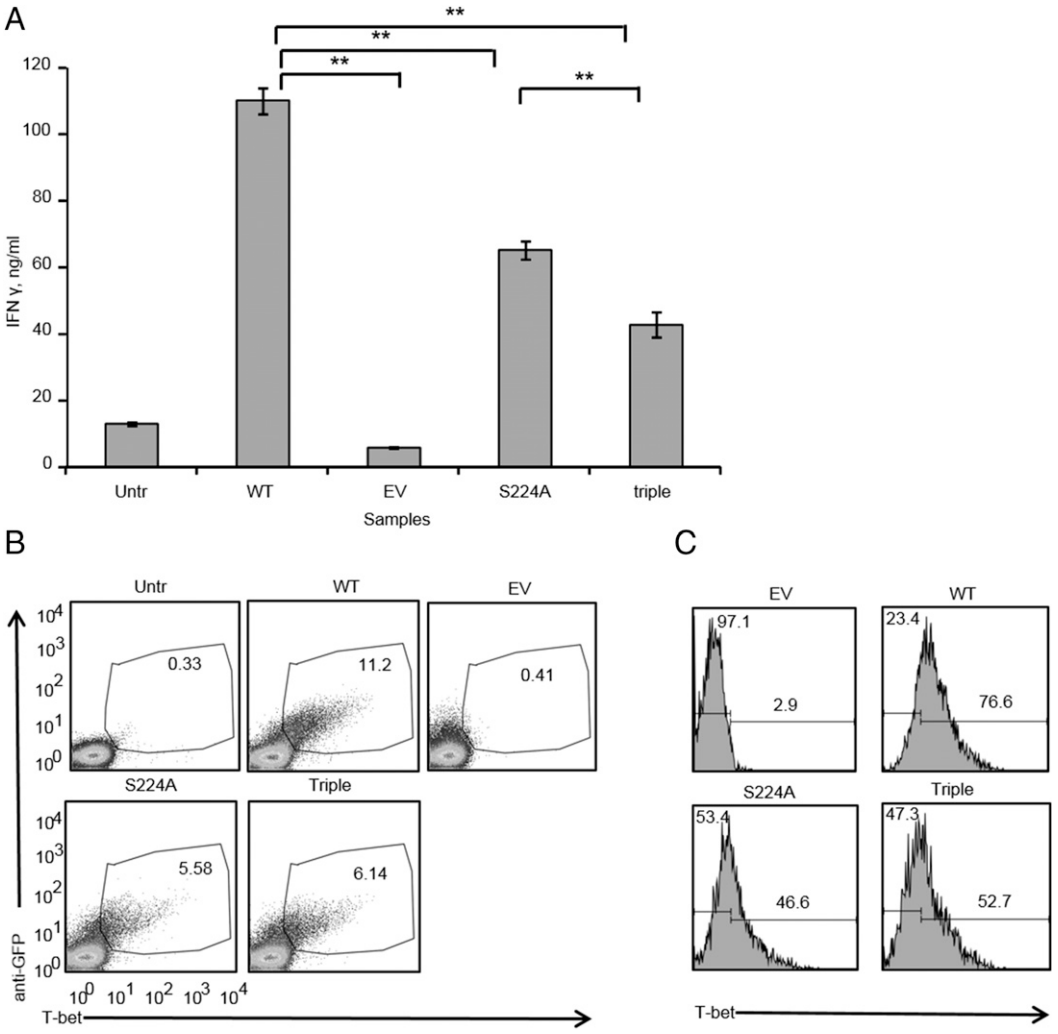


**FIGURE 7.** Triple phosphorylation site T-bet mutant has a significantly reduced ability to induce IFN-γ in T-bet–deficient primary $CD4^+$ T cells. (**A**) $CD4^+$ T cells were purified from spleens and lymph nodes of T-bet–deficient (T-bet KO) mice and transduced with WT, EV, S224A single phosphorylation site mutant, or triple mutant construct containing retroviruses. At 48 h posttransduction equal numbers of $GFP^+$ cells were plated and activated with 1 μg/ml plate-bound anti-CD3 and 2 μg/ml soluble anti-CD28 overnight. Supernatants were analyzed for IFN-γ by ELISA. Error bars are SEM, $^{**}p < 0.05$ by one-way ANOVA with Bonferroni multiple comparison test. (**B**) T-bet KO $CD4^+$ T cells transduced with the constructs indicated in (A) were fixed, permeabilized, and stained with anti-GFP and anti–T-bet Abs. (**C**) Samples from (B) gated on $GFP^+$ cells and T-bet levels are shown as histograms. Data are from one of two experiments with T cells from four individual mice.

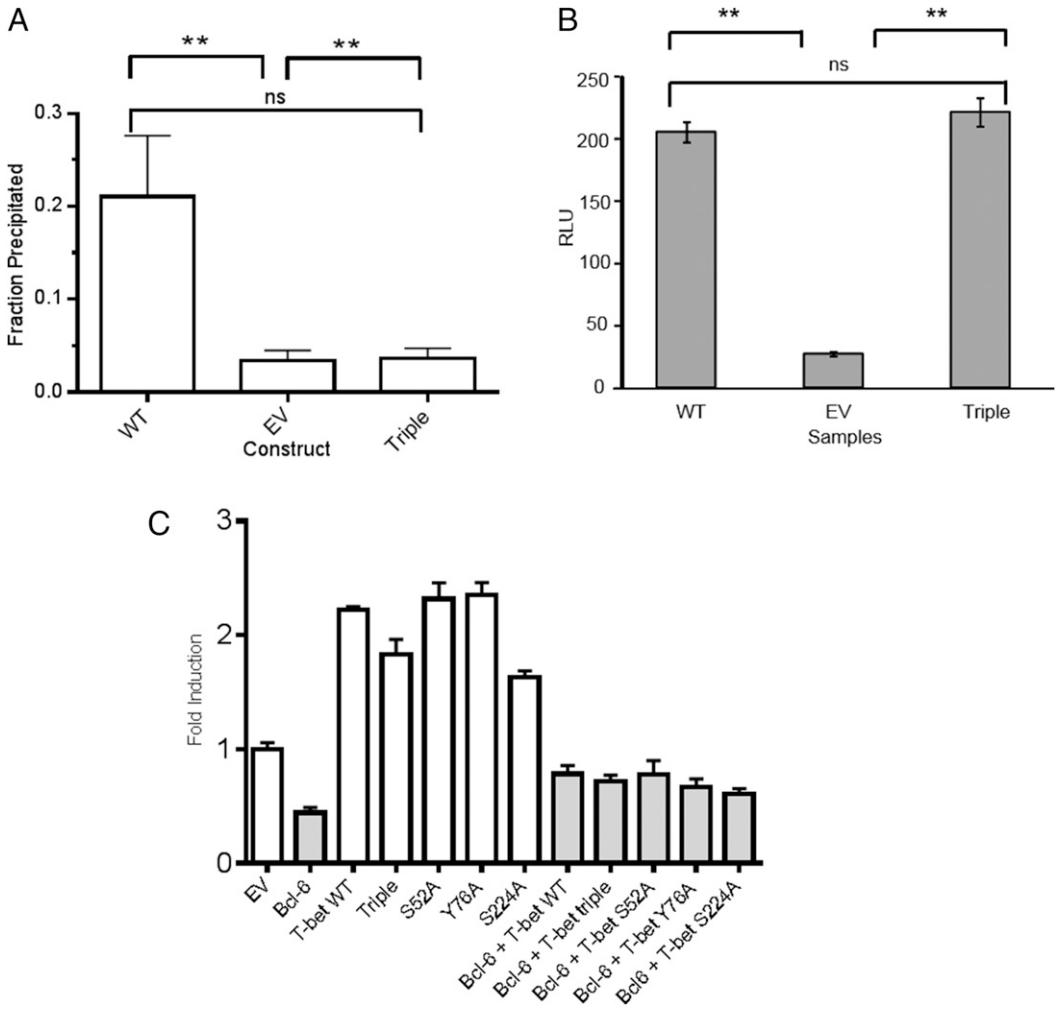


**FIGURE 8.** Triple mutant T-bet has a reduced ability to promote addition of permissive chromatin-remodeling mark H3K4Me2 but can still bind to the *Ifng* and SOCS3 promoters. (**A**) EL4 cells were transiently transfected with EV, WT T-bet, or T-bet triple mutant, and chromatin was fixed after 72 h and sonicated for ChIP. Graph depicts fraction of input DNA precipitated by anti-H3K4Me2–specific Ab from each sample, mean ± SD, $n = 3$ replicates. $^{**}p < 0.05$ by one-way ANOVA with Bonferroni multiple comparison test. Control rabbit IgG precipitated a negligible amount of input and is not shown. The experiment was performed three times with similar results. (**B**) EL4 cells were cotransfected with the pGL3 *Ifng* promoter-reporter construct, pRLtk Renilla control, and with WT T-bet, triple mutant T-bet, or EV. After PMA/ionomycin stimulation, firefly luciferase activity was normalized to the activity of cotransfected Renilla control. Graph depicts relative luminescence units (RLU). Data are from one of two experiments. Error bars are SD, $^{**}p < 0.05$ by one-way ANOVA with Bonferroni multiple comparison test. (**C**) EL4 were cotransfected with the SOCS3 luciferase promoter-reporter construct and EV or T-bet constructs in the absence (open bars) or the presence (gray bars) of Bcl-6. After PMA/ionomycin stimulation, firefly luciferase activity was normalized to cotransfected Renilla luciferase activity and is depicted as fold induction compared with EV. Error bars depict SD, and data are representative of four independent experiments.

induced by T-bet in primary $CD4^+$ T cells (29, 33–35). ChIP using H3K4Me2 Ab demonstrated that the triple mutant T-bet has a significantly reduced ability to promote addition of the permissive histone methylation mark at *Ifng* promoter region (Fig. 8A). Alternatively, the *Ifng* promoter-driven luciferase reporter assay, which is not regulated at the epigenetic level, can be used as a measure of T-bet's ability to bind DNA at a target promoter independently of chromatin-remodeling events (33). By this measure, the triple mutant T-bet's ability to bind DNA at the *Ifng* promoter region was intact (Fig. 8B). It has been demonstrated that T-bet interacts with the Bcl-6 transcription factor. The T-bet/Bcl-6 complex attenuates the expression of T-bet target genes instead of upregulating them (29). Bcl-6 binding to T-bet has shown to take place at the C terminus of T-bet. One of the phosphorylations that we investigated is S508 phosphorylation site and it is located with the C-terminal region of T-bet that has been shown to interact with Bcl-6 (29, 35). We investigated whether novel T-bet phosphorylations we identified impact T-bet's ability to interact with Bcl-6 by cotransfecting T-bet and Bcl-6 into EL4 and monitoring induction of SOCS3 transcription via SOCS3 luciferase promoter-reporter assay. Neither the single phosphorylation mutants nor the triple mutant impacted T-bet's ability to interact with Bcl-6 as shown by the same degree of SOCS3 reporter inhibition for EL4 cotransfected with either WT or mutant T-bet and Bcl-6 (Fig. 8C). Of note, T-bet and Bcl-6 protein levels were similar between the different conditions used for the SOCS3 reporter assay (Supplemental Fig. 4). Together these results demonstrate that triple mutant T-bet can bind DNA and interact with Bcl-6 but has an impaired ability to induce IFN-γ expression due to reduction in its capacity to promote an appropriate permissive epigenetic environment.

## Discussion

In the current study we have identified five novel T-bet phosphorylation sites and demonstrate that four of these phosphory-

lations (S52, Y76, S224, and S508) are mTORC1 dependent. By demonstrating that three of the mTORC1-dependent phosphorylations regulate T-bet's ability to induce IFN-γ expression, our data suggest that mTORC1 controls T-bet's activity in part through a set of phosphorylations. Simultaneous mutations of all three phosphorylation sites into alanine significantly diminished the ability of T-bet to induce IFN-γ expression in both the murine thymoma cell line EL4 and primary T-bet KO $CD4^+$ T cells. Furthermore, we demonstrate that the reduced ability of the triple mutant to induce IFN-γ expression is due in part to its diminished capacity to promote addition of the permissive chromatin mark H3K4Me2 to the *Ifng* promoter region. Although mutating each of the sites individually did not seem to affect IFN-γ production in a transiently transfected cell line, this does not rule out their potential involvement in promoting IFN-γ transcription. Indeed, in experiments employing stable transfection of single mutants in EL4 cells, some single mutants also resulted in decreased IFN-γ when compared with transfection with WT T-bet (data not shown).

T-bet is a member of the T-box protein family of transcription factors, which have been shown to play important roles in cell proliferation, embryogenesis, and organ development. The T-box protein family is characterized by the presence of a highly conserved T-box region that spans ∼200 aa (32). The T-box region is the DNA-binding domain of T-box transcription factors through which T-box transcription factors bind to promoter elements and induce expression of target genes. Only one of the phosphorylation sites discovered in this study (S224) is located within T-bet's T-box DNA-binding domain. Although S224 phosphorylation is mTORC1 dependent, T-bet's ability to bind DNA, as measured by its similar IFN-γ induction compared with WT T-bet, is not diminished in the absence of S224 phosphorylation. The selectivity of our findings is further enhanced by the observation that although the triple mutant abrogated IFN-γ production, it did not affect the ability of T-bet to facilitate Bcl-6–mediated inhibition of T-bet–dependent SOCS3 promoter transcription.

Previously three other T-bet phosphorylation sites within the T-box region (Y219/Y265/Y304) have been demonstrated to be crucial for T-bet's ability to bind DNA proximal to its target genes (16). T-bet promotes the expression of its target genes via two mechanisms. The first mechanism is through T-bet directly binding to the consensus sequence in its target gene's promoter or enhancer region and recruiting transcription machinery, and the second is through recruiting chromatin-remodeling complexes to its target gene promoter and facilitating the addition of permissive and removal of prohibitive chromatin-remodeling marks (11, 32–34, 36). Studies from the Weinmann laboratory (32–34) have demonstrated that T-bet regions that are responsible for recruitment of chromatin-remodeling complexes are predominantly located on the N terminus of T-bet and overlap with T-box DNA-binding domain. Therefore, we hypothesized that S224, S52, and Y76 mTORC1-dependent phosphorylations discovered in this study could be important for recruiting chromatin-remodeling complexes. Our data supports this hypothesis by demonstrating that a triple mutant T-bet binds to and activates an *Ifng* promoter-reporter construct but has a reduced ability to promote the addition of the H3K4Me2 permissive chromatin mark to the endogenous *Ifng* promoter region within chromatin.

Y219/Y265/Y304 phosphorylations that regulate T-bet's DNA binding and ability to promote Th1 differentiation are imparted onto T-bet by c-Abl tyrosine kinase (16). Among the novel mTORC1-dependent phosphorylation sites discovered in this study, there are both serine (S52, S224) and tyrosine (Y76) phosphorylation. Therefore, these phosphorylations may be imparted onto T-bet by two distinct kinases, one with serine/threonine specificity and another with tyrosine specificity, or a dual-specificity kinase. Such findings suggest that at least some of the phosphorylation sites we identified are not direct substrates of mTORC1, despite the regulation of their phosphorylation state by mTORC1 activity. Although identification of the kinases that directly phosphorylate the T-bet residues that we identified is beyond the scope of this work, preliminary immunoprecipitation studies have identified interactions between mTORC1 and several dual-specificity protein kinases. The capacity of these kinases to phosphorylate T-bet on the sites we identified remains under investigation.

Interestingly, four out of five novel phosphorylation sites in mouse T-bet protein discovered in this study are present in human T-bet. Previous studies from our laboratory (37) have demonstrated that mTOR regulates human $CD4^+$ T cell effector differentiation. Thus, we predict that mTORC1 regulates T-bet function via phosphorylation not only in mouse $CD4^+$ T cells but in human $CD4^+$ T cells as well.

## Acknowledgments

We thank Dr. Stefani Thomas and Dr. Elisabeth Hersman for help with designing and implementing LC-MRM-MS assays for phosphorylated peptides. We thank Jiayu Wen and Chirag Patel from Dr. Jonathan Powell's laboratory for help with managing mouse strain colonies used for this study. We thank Hong Sun, Minhee Oh, and Chirag Patel from the Powell laboratory for input on manuscript writing and on design assays for T-bet function in primary $CD4^+$ T cells. We also thank Dr. Aki Furusawa from Dr. Arnob Banerjee's laboratory for help with optimizing retroviral transduction of T-bet KO $CD4^+$ T cells and providing us with spleens and lymph nodes of T-bet KO mice. We thank Dr. Amy Weinmann from University of Alabama at Birmingham for help with designing H3K4Me2 ChIP and for kindly giving us the Bcl-6 expression construct as well as SOCS3 and IFN-γ luciferase reporter constructs.

## Disclosures

The authors have no financial conflicts of interest.

## References

1. Wan, Y. Y. 2010. Multi-tasking of helper T cells. *Immunology* 130: 166–171.
2. Lucas, S., N. Ghilardi, J. Li, and F. J. de Sauvage. 2003. IL-27 regulates IL-12 responsiveness of naive CD4+ T cells through Stat1-dependent and -independent mechanisms. *Proc. Natl. Acad. Sci. USA* 100: 15047–15052.
3. Szabo, S. J., S. T. Kim, G. L. Costa, X. Zhang, C. G. Fathman, and L. H. Glimcher. 2000. A novel transcription factor, T-bet, directs Th1 lineage commitment. *Cell* 100: 655–669.
4. Lazarevic, V., and L. H. Glimcher. 2011. T-bet in disease. *Nat. Immunol.* 12: 597–606.
5. Delgoffe, G. M., T. P. Kole, Y. Zheng, P. E. Zarek, K. L. Matthews, B. Xiao, P. F. Worley, S. C. Kozma, and J. D. Powell. 2009. The mTOR kinase differentially regulates effector and regulatory T cell lineage commitment. *Immunity* 30: 832–844.
6. Delgoffe, G. M., K. N. Pollizzi, A. T. Waickman, E. Heikamp, D. J. Meyers, M. R. Horton, B. Xiao, P. F. Worley, and J. D. Powell. 2011. The kinase mTOR regulates the differentiation of helper T cells through the selective activation of signaling by mTORC1 and mTORC2. *Nat. Immunol.*
7. Powell, J. D., and G. M. Delgoffe. 2010. The mammalian target of rapamycin: linking T cell differentiation, function, and metabolism. *Immunity* 33: 301–311.
8. Laplante, M., and D. M. Sabatini. 2012. mTOR Signaling. *Cold Spring Harb. Perspect. Biol.* 4: a011593.
9. Yang, K., S. Shrestha, H. Zeng, P. W. Karmaus, G. Neale, P. Vogel, D. A. Guertin, R. F. Lamb, and H. Chi. 2013. T cell exit from quiescence and differentiation into Th2 cells depend on Raptor-mTORC1-mediated metabolic reprogramming. *Immunity* 39: 1043–1056.
10. Zeng, H., K. Yang, C. Cloer, G. Neale, P. Vogel, and H. Chi. 2013. mTORC1 couples immune signals and metabolic programming to establish T(reg)-cell function. *Nature* 499: 485–490.
11. Miller, S. A., and A. S. Weinmann. 2010. Molecular mechanisms by which T-bet regulates T-helper cell commitment. *Immunol. Rev.* 238: 233–246.
12. Plevy, S. E., C. J. Landers, J. Prehn, N. M. Carramanzana, R. L. Deem, D. Shealy, and S. R. Targan. 1997. A role for TNF-alpha and mucosal T helper-1 cytokines in the pathogenesis of Crohn's disease. *J. Immunol.* 159: 6276–6282.

13. Oh, S., and E. S. Hwang. 2014. The role of protein modifications of T-bet in cytokine production and differentiation of T helper cells. *J. Immunol. Res.* 2014: 589672.
14. Jang, E. J., H. R. Park, J. H. Hong, and E. S. Hwang. 2013. Lysine 313 of T-box is crucial for modulation of protein stability, DNA binding, and threonine phosphorylation of T-bet. *J. Immunol.* 190: 5764–5770.
15. Hwang, E. S., J. H. Hong, and L. H. Glimcher. 2005. IL-2 production in developing Th1 cells is regulated by heterodimerization of RelA and T-bet and requires T-bet serine residue 508. *J. Exp. Med.* 202: 1289–1300.
16. Chen, A., S. M. Lee, B. Gao, S. Shannon, Z. Zhu, and D. Fang. 2011. c-Abl-mediated tyrosine phosphorylation of the T-bet DNA-binding domain regulates CD4+ T-cell differentiation and allergic lung inflammation. *Mol. Cell. Biol.* 31: 3445–3456.
17. Lazarevic, V., X. Chen, J. H. Shim, E. S. Hwang, E. Jang, A. N. Bolm, M. Oukka, V. K. Kuchroo, and L. H. Glimcher. 2011. T-bet represses T(H)17 differentiation by preventing Runx1-mediated activation of the gene encoding RORγt. *Nat. Immunol.* 12: 96–104.
18. Cutillas, P. R. 2015. Role of phosphoproteomics in the development of personalized cancer therapies. *Proteomics Clin. Appl.* 9: 383–395.
19. Gillette, M. A., and S. A. Carr. 2013. Quantitative analysis of peptides and proteins in biomedicine by targeted mass spectrometry. *Nat. Methods* 10: 28–34.
20. Picotti, P., B. Bodenmiller, and R. Aebersold. 2013. Proteomics meets the scientific method. *Nat. Methods* 10: 24–27.
21. Yee, W. M., and P. F. Worley. 1997. Rheb interacts with Raf-1 kinase and may function to integrate growth factor- and protein kinase A-dependent signals. *Mol. Cell. Biol.* 17: 921–933.
22. Mottaz-Brewer, H. M., A. D. Norbeck, J. N. Adkins, N. P. Manes, C. Ansong, L. Shi, Y. Rikihisa, T. Kikuchi, S. W. Wong, R. D. Estep, et al. 2008. Optimization of proteomic sample preparation procedures for comprehensive protein characterization of pathogenic systems. *J. Biomol. Tech.* 19: 285–295.
23. MacLean, B., D. M. Tomazela, N. Shulman, M. Chambers, G. L. Finney, B. Frewen, R. Kern, D. L. Tabb, D. C. Liebler, and M. J. MacCoss. 2010. Skyline: an open source document editor for creating and analyzing targeted proteomics experiments. *Bioinformatics* 26: 966–968.
24. Hersman, E. M., and N. N. Bumpus. 2014. A targeted proteomics approach for profiling murine cytochrome P450 expression. *J. Pharmacol. Exp. Ther.* 349: 221–228.
25. Gray, C. M., and M. J. May. 2015. Stable reconstitution of IKK-deficient mouse embryonic fibroblasts. *Methods Mol. Biol.* 1280: 181–195.
26. Furusawa, A., K. Sadashivaiah, Z. N. Singh, C. I. Civin, and A. Banerjee. 2016. Inefficient megakaryopoiesis in mouse hematopoietic stem-progenitor cells lacking T-bet. *Exp. Hematol.* 44: 194–206.e117.
27. Pear, W. S., G. P. Nolan, M. L. Scott, and D. Baltimore. 1993. Production of high-titer helper-free retroviruses by transient transfection. *Proc. Natl. Acad. Sci. USA* 90: 8392–8396.
28. Song, C., K. Sadashivaiah, A. Furusawa, E. Davila, K. Tamada, and A. Banerjee. 2014. Eomesodermin is required for antitumor immunity mediated by 4-1BB-agonist immunotherapy. *OncoImmunology* 3: e27680.
29. Oestreich, K. J., A. C. Huang, and A. S. Weinmann. 2011. The lineage-defining factors T-bet and Bcl-6 collaborate to regulate Th1 gene expression patterns. *J. Exp. Med.* 208: 1001–1013.
30. Blom, N., S. Gammeltoft, and S. Brunak. 1999. Sequence and structure-based prediction of eukaryotic protein phosphorylation sites. *J. Mol. Biol.* 294: 1351–1362.
31. Hwang, E. S., S. J. Szabo, P. L. Schwartzberg, and L. H. Glimcher. 2005. T helper cell fate specified by kinase-mediated interaction of T-bet with GATA-3. *Science* 307: 430–433.
32. Lewis, M. D., S. A. Miller, M. M. Miazgowicz, K. M. Beima, and A. S. Weinmann. 2007. T-bet's ability to regulate individual target genes requires the conserved T-box domain to recruit histone methyltransferase activity and a separate family member-specific transactivation domain. *Mol. Cell. Biol.* 27: 8510–8521.
33. Miller, S. A., A. C. Huang, M. M. Miazgowicz, M. M. Brassil, and A. S. Weinmann. 2008. Coordinated but physically separable interaction with H3K27-demethylase and H3K4-methyltransferase activities are required for T-box protein-mediated activation of developmental gene expression. *Genes Dev.* 22: 2980–2993.
34. Miller, S. A., S. E. Mohn, and A. S. Weinmann. 2010. Jmjd3 and UTX play a demethylase-independent role in chromatin remodeling to regulate T-box family member-dependent gene expression. *Mol. Cell* 40: 594–605.
35. Oestreich, K. J., K. A. Read, S. E. Gilbertson, K. P. Hough, P. W. McDonald, V. Krishnamoorthy, and A. S. Weinmann. 2014. Bcl-6 directly represses the gene program of the glycolysis pathway. *Nat. Immunol.* 15: 957–964.
36. Oestreich, K. J., and A. S. Weinmann. 2012. Transcriptional mechanisms that regulate T helper 1 cell differentiation. *Curr. Opin. Immunol.* 24: 191–195.
37. Pollizzi, K. N., A. T. Waickman, C. H. Patel, I. H. Sun, and J. D. Powell. 2015. Cellular size as a means of tracking mTOR activity and cell fate of CD4+ T cells upon antigen recognition. *PLoS One* 10: e0121710.